

# Planetary companions around the metal-poor star HIP 11952

J. Setiawan<sup>1</sup>, V. Roccatagliata<sup>2,1</sup>, D. Fedele<sup>3</sup>, Th. Henning<sup>1</sup>, A. Pasquali<sup>4</sup>, M.V. Rodríguez-Ledesma<sup>1,5</sup>, E. Caffau<sup>4</sup>, U. Seemann<sup>5,6</sup>, and R.J. Klement<sup>7,1</sup>

<sup>1</sup> Max-Planck-Institut für Astronomie, Königstuhl 17, D-69117 Heidelberg, Germany  
e-mail: setiawan@mpia.de

<sup>2</sup> Space Telescope Science Institute, 3700 San Martin Drive, Baltimore, MD 21218, USA

<sup>3</sup> Department of Physics and Astronomy, Johns Hopkins University, 3400 North Charles Street, Baltimore, MD 21218, USA

<sup>4</sup> Astronomisches Rechen-Institut, Zentrum für Astronomie, Mönchhofstrasse, 12-14, D-69120, Heidelberg

<sup>5</sup> Institut für Astrophysik, Georg-August-Universität, Friedrich-Hund-Platz 1, D-37077 Göttingen, Germany

<sup>6</sup> European Southern Observatory, Karl-Schwarzschild Str. 2, D-85748, Garching bei München, Germany

<sup>7</sup> University of Würzburg, Department of Radiation Oncology, D-97080 Würzburg, Germany

Received 4/8/2011 - Accepted 27/2/2012

## ABSTRACT

**Aims.** We carried out a radial-velocity survey to search for planets around metal-poor stars. In this paper we report the discovery of two planets around HIP 11952, a metal-poor star with  $[\text{Fe}/\text{H}] = -1.9$  that belongs to our target sample.

**Methods.** Radial velocity variations of HIP 11952 were monitored systematically with FEROS at the 2.2 m telescope located at the ESO La Silla observatory from August 2009 until January 2011. We used a cross-correlation technique to measure the stellar radial velocities (RV).

**Results.** We detected a long-period RV variation of 290 d and a short-period one of 6.95 d. The spectroscopic analysis of the stellar activity reveals a stellar rotation period of 4.8 d. The Hipparcos photometry data shows intra-day variabilities, which give evidence for stellar pulsations. Based on our analysis, the observed RV variations are most likely caused by the presence of unseen planetary companions. Assuming a primary mass of  $0.83 M_{\odot}$ , we computed minimum planetary masses of  $0.78 M_{\text{Jup}}$  for the inner and  $2.93 M_{\text{Jup}}$  for the outer planet. The semi-major axes are  $a_1 = 0.07$  AU and  $a_2 = 0.81$  AU, respectively.

**Conclusions.** HIP 11952 is one of very few stars with  $[\text{Fe}/\text{H}] < -1.0$  which have planetary companions. This discovery is important to understand planet formation around metal-poor stars.

**Key words.** star: general – star: individual: HIP 11952 – planetary system – technique: radial velocity

## 1. Introduction

Current results of the exoplanet surveys strongly suggest a correlation between a star's stellar metallicity and its probability of hosting planets, in particular for main-sequence stars (e.g., Fischer & Valenti 2005; Johnson et al. 2010). According to these studies, the detection rate of planets decreases with metallicity. However, the conclusions of Fischer & Valenti (2005) might be affected by an observational bias, since these authors did not have similar numbers of stars in their survey per bin of metallicity. Therefore, it is crucial to understand if either the high stellar metallicity triggers planet formation or the metal enhancement of stars is caused by the formation of planets.

In the last years, exoplanet surveys tried to bridge this gap, starting to include more metal-poor stars in their samples. Sozzetti et al. (2009) conducted a three-year RV survey to look for planets around metal-poor stars down to  $[\text{Fe}/\text{H}] = -2.0$  and found no evidence for short-period giant planets within 2 AU from the central star. Santos et al. (2011) performed a similar survey, only down to  $[\text{Fe}/\text{H}] = -1.4$  and found three moderately

metal-poor stars hosting a long period giant planets ( $P > 700$  d). A hot Saturn and a hot Jupiter have been found transiting two moderate metal-poor stars, with  $[\text{Fe}/\text{H}] = -0.46$  and  $-0.4$ , respectively (Bouchy et al. 2010; Simpson et al. 2011).

In June 2009 we started a survey to search for planets around metal-poor stars. The target sample includes 96 metal-poor A and F stars. Our target list includes stars with metallicities in the range  $-4.0 \leq [\text{Fe}/\text{H}] \leq -0.5$ . As part of this work, Setiawan et al. (2010) found a planet around an extremely metal-poor red horizontal branch star with a short period of 16.2 d. We notice that its  $[\text{Fe}/\text{H}] = -2.1$  is not included in the metallicity range covered by the surveys of Sozzetti et al. (2009) and Santos et al. (2011).

These recent observations have started to disclose the realm of planets at rather low stellar metallicities, indicating that metallicity may not be the main driver of planet formation. Clearly, more statistics is needed to obtain robust conclusions. In this framework, we report the detection of two planetary companions around HIP 11952 as a result of our RV planet survey around metal-poor stars.

Send offprint requests to: J. Setiawan

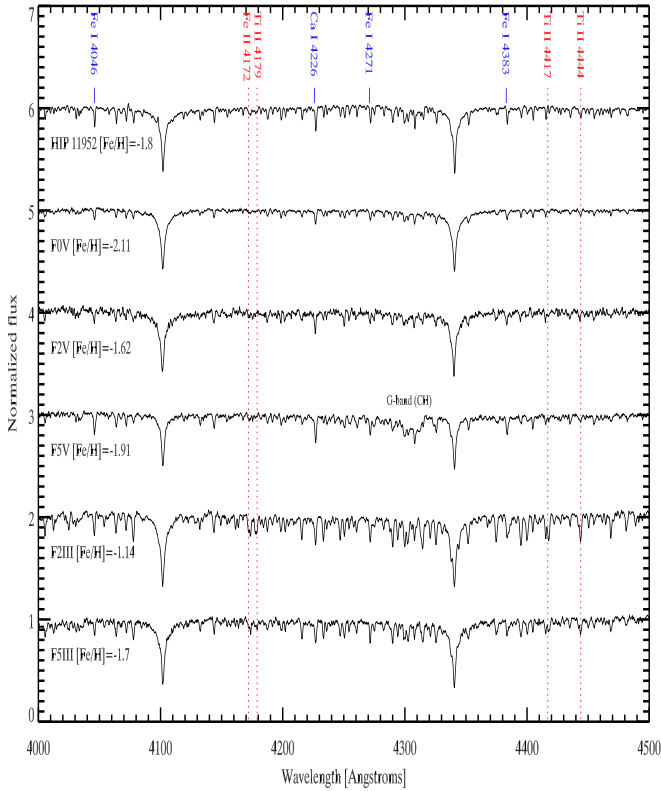


**Fig. 1.** Comparison of the spectrum of HIP 11952 with stellar spectra of the Indo-US library. The dashed lines highlight some iron lines (Fe II, Ti II) which are sensitive to the luminosity class of the star. The solid lines in the upper part of the figure indicate the position of some iron and calcium lines which do not vary with the luminosity class.

The paper is organized as follows: Observations and data reduction are presented in section 2. The stellar parameters of HIP 11952 are shown in section 3.1 together with the most relevant information available for this star in the literature. In section 3.2 we describe the RV and photometric analysis. The detection of the planetary companion is addressed in section 4. Discussion and conclusions are given in sections 5 and 6, respectively.

## 2. Observations and data reduction

We observed HIP 11952 from August 2009 until January 2011 with FEROS at the 2.2 m Max-Planck Gesellschaft/European Southern Observatory (MPG/ESO) telescope, located at ESO-La Silla observatory, during the MPG guarantee time. FEROS has a resolution of  $R = 48\,000$  and a wavelength coverage of 370–920 nm (Kaufer & Pasquini 1998). The long-term RV precision of FEROS was measured across a period of 6 years, from December 2003 until January 2010, using the standard star  $\tau$  Ceti (HD 10700). We obtained an RV precision of better than  $11 \text{ m s}^{-1}$ .

The data reduction was performed with a software package in the ESO-MIDAS environment available online at the telescope. The procedure of the RV computation from the FEROS spectra is described in Setiawan et al. (2003) and based on a cross-correlation technique. The spectra of HIP 11952 were

cross-correlated with a template of an F dwarf star which best matches the spectral type of HIP 11952.

## 3. Analysis

In this section we present the analysis of the stellar parameters and RVs derived from the FEROS spectra.

### 3.1. The star HIP 11952

HIP 11952 (HD 16031; LP 710-89) was previously classified as an F0 dwarf star (e.g., Wright et al. 2003; Kharchenko & Roeser 2009) and as a giant G8 (e.g. Sánchez-Blázquez et al. 2006; Cenarro et al. 2007).

Our spectral classification was carried out by comparing the FEROS spectrum of HIP 11952 with spectra from the Indo-US library (Valdes et al. 2004) of metal-poor stars with different luminosity classes and spectral types. The FEROS spectrum was convolved to the resolution of the Indo-US spectral library ( $1\text{Å}$ ). Following the spectral classification criteria presented by Gray & Corbally (2009), we used some lines (Fe II, Ti II) which are sensitive to the luminosity class of the star as well as other iron (Fe I) and calcium (Ca I) lines which do not vary with the luminosity class (Fig. 1). From this comparison we concluded that HIP 11952 is an F2V star. However, this result has to be confirmed by an independent spectroscopic analysis of the stellar spectra, as we present below.

HIP 11952 is at a distance of 115.3 pc as derived from the parallax measurements given in the Hipparcos catalogue (Perryman 1997). Fundamental parameters of this star were determined using our high-resolution FEROS spectra. In particular, stellar abundances, effective temperature and surface gravity were computed using the synthetic spectra from the 1D ATLAS models (Kurucz 1993; Kurucz 2005) and the fit of the  $H\alpha$  line to the CO5BOLD 3D model atmosphere (Caffau et al. 2011). The atomic data of the iron lines are from the Large Program “First Stars” lead by R. Cayrel, optimized for metal-poor stars (see Sivarani et al. 2004). The first attempt of abundance analysis was based on 1D ATLAS model atmospheres computed using the version 9 of the code ATLAS (Kurucz 1993; Kurucz 2005) running under Linux (Sbordone et al. 2004; Sbordone 2005). We derived a temperature of 5960 K by fitting the  $H\alpha$  wings with a grid of synthetic spectra computed from ATLAS models, and a temperature of 6120 K when we used a grid of synthetic spectra based on 3D models.

By imposing an agreement between the iron abundance derived from the lines of Fe I and the lines of Fe II, we derived surface gravities  $\log g$  of 3.8 and 4.0 for the two cases of  $T_{\text{eff}} = 5960 \text{ K}$  and  $6120 \text{ K}$ , respectively. The uncertainty on the effective temperature derived from the fit of the  $H\alpha$  is 150 K, while the error in the surface gravity is 0.3. A microturbulence of  $1.4 \text{ km s}^{-1}$  was derived by minimizing the slope of the abundance versus equivalent width (EW) relation. The resulting iron abundance derived is  $[\text{Fe}/\text{H}] = -1.95 \pm 0.09$  for  $T_{\text{eff}} = 5960 \text{ K}$  and  $[\text{Fe}/\text{H}] = -1.85 \pm 0.09$  for  $T_{\text{eff}} = 6120 \text{ K}$ , respectively.

We thus obtained two possible parameter sets for this star:  $(T_{\text{eff}}, \log g, [\text{Fe}/\text{H}]) = (5960 \text{ K}, 3.8, -1.95)$  (1D ATLAS) and  $(6120 \text{ K}, 4.0, -1.85)$  (3D MODELS). We measured an  $\text{EW} = 3.07 \pm 0.03 \text{ mÅ}$  of the Li feature at 670.7 nm, which implies an abundance  $A(\text{Li}) = 2.2$  if we fix  $T_{\text{eff}} = 6120 \text{ K}$ , and  $A(\text{Li}) = 2.1$  in the case  $T_{\text{eff}} = 5960 \text{ K}$ .

Feltzing et al. (2001) derived a stellar age of  $12.8 \pm 2.6 \text{ Gyr}$  by comparing the Strömgen photometry of HIP 11952 with

the evolutionary tracks computed for the Strömgen metallicity ( $[m/H] = -1.54$ ) of the star. We checked their result using the photometry provided by Hipparcos for HIP 11952 in the Bessell filters system (Bessell 2000) with the isochrones by Marigo et al. (2008) and Girardi et al. (2010), calculated for the Strömgen metallicity of the star. In the assumption that the dust extinction along the line of sight to HIP 11952 is not large, the Hipparcos photometry indicates, within its uncertainty, an age older than 10 Gyr for this star.

We used the isochrones by Marigo et al. (2008) and Girardi et al. (2010) computed for  $[m/H] = -1.54$  and ages in the range 10–13 Gyr in order to consistently derive the mass and radius of HIP 11952. By comparing its photometry with the selected isochrones, we constrained its mass between  $0.79 M_{\odot}$  and  $0.88 M_{\odot}$ . From the relation between surface gravity, stellar mass and stellar radius:

$$\frac{R}{R_{\odot}} = \sqrt{\frac{M}{M_{\odot}} \frac{g_{\odot}}{g}} \quad (1)$$

we derived a stellar radius of  $1.6 \pm 0.1 R_{\odot}$ , where the error is obtained from the errors propagation. The derived stellar mass and radius adopted in this work are:  $0.83^{+0.05}_{-0.04} M_{\odot}$  and  $1.6 \pm 0.1 R_{\odot}$ .

Fundamental stellar parameters have also been estimated in previous studies (e.g., Masana et al. 2006; Charbonnel et al. 2005). The corresponding values are  $T_{\text{eff}} = 6367$  K, a stellar radius  $R_{*} = 1.0 R_{\odot}$  and surface gravity  $\log g = 4.1$ . Feltzing et al. (2001) reported  $m = 0.785 M_{\odot}$ . If we compile all literature values for the surface gravity given in Cayrel de Strobel et al. (2001) and use  $R_{*} = 1.0 R_{\odot}$ , we obtain a mean value  $m = 0.55 \pm 0.23 M_{\odot}$ . Within the errors, these values are consistent with those we derived, although the stellar radius is smaller than the one we adopted. Finally, we compared the derived stellar parameters with those given by Casagrande et al. (2010). These authors measured  $\log g = 4.17$ ,  $[Fe/H] = -1.74$  and  $T_{\text{eff}} = 6186$  K. Within the uncertainties, these values are in good agreement with our determination.

Based on the surface gravity and radius derived from our analysis and the available literature data, HIP 11952 is more likely a star already evolved off the main-sequence, roughly sitting at the base of the subgiant branch.

Astrometric and photometric data of HIP 11952 can be found in public catalogues (e.g., Hipparcos). The astrometric variability is less than 5 mas, allowing the conclusion that an unseen stellar companion in the system can be ruled out. Nevertheless, older RV measurements from Eggen & Sandage (1959) combined with Carney & Latham (1987) suggested that HIP 11952 may be a spectroscopic binary SB1 (Fouts 1987). However, our measurements can neither reject nor confirm this claim yet. The updated parameters of HIP 11952 are given in Table 1.

HIP 11952 is listed as a member of the metal-poor stellar stream detected by Arifanto & Fuchs (2006), a group of putative thick disk stars moving on similar orbits in the Galactic potential and currently lagging the Local Standard of Rest by  $V_{\text{lag}} \approx 80 \text{ km s}^{-1}$ . As such, HIP 11952 might stem from one of the Milky Way's former satellite galaxies that once got tidally disrupted. Alternatively, Minchev et al. (2009) showed that the stream might consist of *in situ* disk stars being scattered towards common orbits through a merger-induced perturbation of the old disk  $\sim 1.9$  Gyr ago. It is also possible that there is a connection to the Arcturus stream at  $V_{\text{lag}} \approx 100$  which itself could have a tidal or a dynamical origin (see discussion in Klement (2010) for more details).

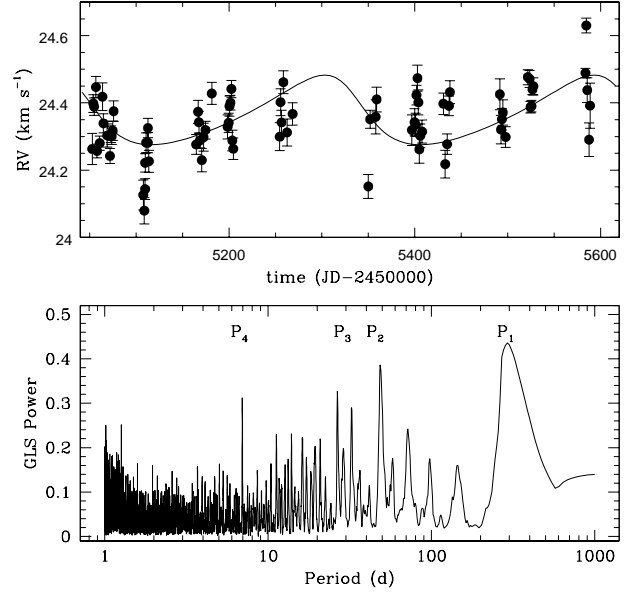


**Fig. 2.** RV observations of HIP 11952, taken with FEROS from August 2009 until January 2011 (upper panel). We calculated a single Keplerian fit to the data (solid line) for the outer component. A multi-component Keplerian fit is presented in Fig. 9, see Table. 3. The lower panel shows a Generalized Lomb-Scargle (GLS) periodogram of the whole RV data set. The highest peak, marked with P<sub>1</sub> corresponds to a period of  $290 \pm 16$  d with a False Alarm Probability of  $\sim 7 \times 10^{-6}$ .

**Table 1.** Stellar parameters of HIP 11952

Parameter	value	unit
Spectral type*	F2V – IV	
$m_V^{(a)}$	$9.88 \pm 0.02$	mag
Parallax <sup>(a)</sup>	$8.67 \pm 1.81$	mas
$T_{\text{eff}}^*$	$5960 \pm 150$	K
	$6120 \pm 150$	K
$\log g^*$	$3.8 \pm 0.3$	$\text{cm}^2/\text{g}$
	$4.0 \pm 0.3$	$\text{cm}^2/\text{g}$
$[Fe/H]^*$	$-1.95 \pm 0.09$	dex
	$-1.85 \pm 0.09$	dex
$R_{*}^*$	$1.6 \pm 0.1$	$R_{\odot}$
Mass*	$0.83^{+0.05}_{-0.04}$	$M_{\odot}$
Age <sup>(b)</sup>	$12.8 \pm 2.6$	Gyr
$v_{\text{rot}} \sin i^*$	$5.2 \pm 1.0$	$\text{km s}^{-1}$
$P_{\text{rot}}/\sin i$	$15.7 \pm 2.5$	d

\* this work

<sup>a</sup> Hipparcos catalogue (Perryman 1997)

<sup>b</sup> Feltzing et al. (2001)

### 3.2. Radial velocity

The RV variation of HIP 11952 is shown in Fig. 2 (upper panel). During the observation campaigns we obtained 77 RV measurements (Table. 2). We applied the Generalized Lomb-Scargle (GLS) periodogram (Zechmeister & Kürster 2009) to the RV data in order to search for periodicities.

We found several signals in the periodogram, as shown in the lower panel of Fig. 2. The four highest signals are marked with P<sub>1</sub>, P<sub>2</sub>, P<sub>3</sub> and P<sub>4</sub>. The highest peak P<sub>1</sub> has a False Alarm Probability (FAP) of  $7.2 \times 10^{-6}$  and corresponds to a period of

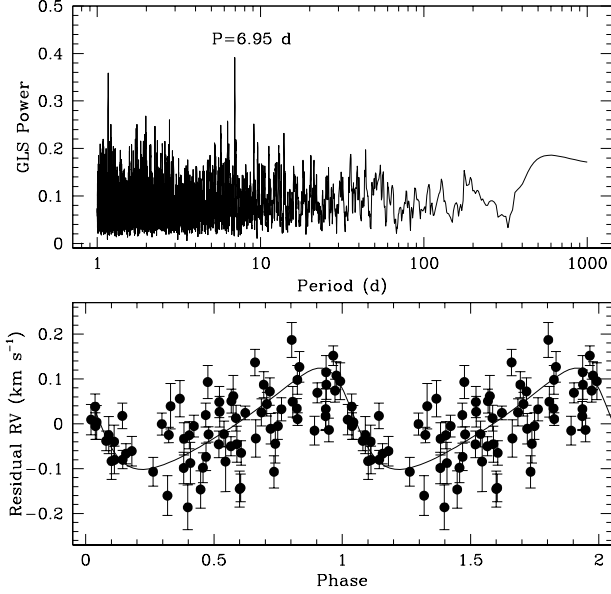


**Fig. 3.** The residual RV after removing the 290 d periodicity. The periodogram in the upper panel shows two peaks at 6.95 d and 1.16 d. The 1.16 d is identified as a harmonic of 6.95 d ( $1/1.16 + 1/6.95 = 1.0$ ). The lower panel shows the phase folded RVs with a period of 6.95 d. The solid line shows a Keplerian fit for the residual RV variation.

$290 \pm 16$  d. We computed a Keplerian fit to the data, shown as the solid line in the upper panel of Fig. 2. The parameters of this fit are given in Table 3.

After removing the 290 d signal, the peaks  $P_2$  and  $P_3$  disappear. However, the peak  $P_4$  remains, which means that this signal is not an alias of  $P_1$ . The signal  $P_4$  corresponds to a period of 6.95 d with  $\text{FAP} = 8 \times 10^{-4}$ . In the residual RV periodogram, we also observed a signal at 1.16 d (Fig. 3 upper panel), which is obviously a harmonic of the 6.95 d period ( $1/6.95 + 1/1.16 = 1.0$ ). In the lower panel of Fig. 3 we have phase folded the RVs with  $P = 6.95$  d and show a Keplerian fit with the parameters listed in Table 3. After excluding stellar activity as the cause for the RV variations in the next sections, we are going to interpret the signals  $P_1$  and  $P_4$  as orbital periods of unseen low-mass companions (section 4 below).

### 3.3. Stellar rotation

A systematic investigation of the stellar activity is mandatory to avoid wrong interpretations of the observed RV variations. There are several possibilities to probe the stellar activity. The line profile asymmetry (bisector) and the Ca II lines are known as reliable stellar activity indicators. These activity indicators, if they show periodic variations, can be used to determine the stellar rotation period. Besides the spectroscopic methods, photometric observations are also commonly used to find the stellar rotation period.

HIP 11952 itself is not a star with high stellar activity. This is inferred from the absence of emission cores in Ca II K ( $\lambda 3934$ ) and H ( $\lambda 3967$ ). Furthermore, no H $\alpha$  emission line was observed in the spectra. The projected rotational velocity is also relatively low ( $v \sin i = 5.2 \text{ km s}^{-1}$ ) compared to other F-type dwarf stars (de Medeiros & Mayor 1999). Finally, using the relation

$P / \sin i = 2\pi R_* / v \sin i$ , the maximum stellar rotation period is found to be  $15.7 \pm 2.5$  d.

#### 3.3.1. Line profile asymmetry

The line profile asymmetry can be quantified by the bisector velocity span (BVS). A definition of the BVS is given, e.g., in Hatzes (1996). We measured the BVS of the stellar spectra and searched for any periodicity that might be related to the RV variation. In the GLS periodogram of BVS we found, however, no significant peak. Thus, we cannot use the bisector to determine the stellar rotation period. We then searched for a correlation between BVS and RV to find out whether the observed RV variation is due to rotational modulation. We computed a correlation coefficient  $c = 0.1$  between the RV and BVS (Fig. 4). This value indicates that the RV variation is not correlated with the BVS. However, it does not give any hint about the stellar rotation period.

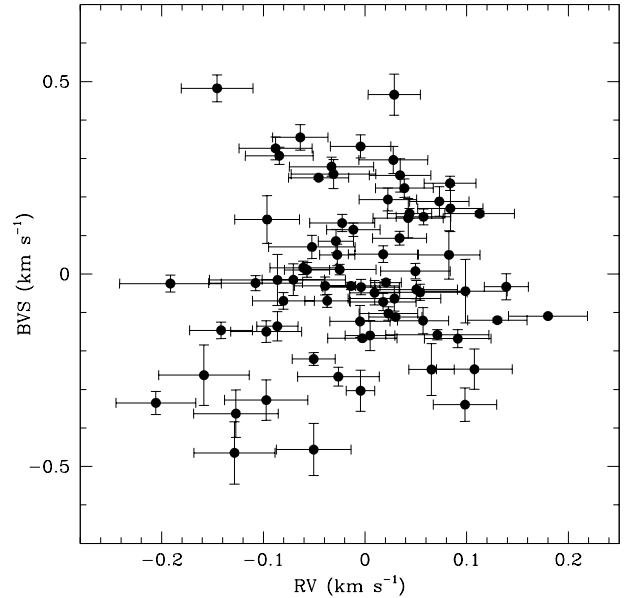


**Fig. 4.** The figure shows the measurements of BVS, plotted against residual RVs. The plot shows no correlation between BVS and RV. We computed a correlation coefficient  $c = 0.1$ .

#### 3.3.2. Ca II analysis

As mentioned before we found no emission cores in the Ca II H & K lines ( $\lambda 3934, 3968$ ) which are, in general, excellent stellar activity indicators to probe the rotational modulation of the star. Nevertheless, we investigated to possibility to use Ca II K lines to find any indication of stellar activity. We calculated the stellar activity index, known as  $S$ -index, similar to the method described in Vaughan et al. (1978) and Santos et al. (2000). We found a significant periodicity of 36 d in the periodogram, but the error bar of the individual measurement is large. This value is also close to the typical observational window of about one month. Thus, also by considering  $P / \sin i$  value, we do not adopt this as the stellar rotation period.

We exploited the capability of FEROS to investigate the Ca II lines  $\lambda 8498, 8662$ , following the technique presented e.g. by

**Table 2.** RV variation of HIP 11952

JD	RV	error	JD	RV	error
-2450000	(m/s)	(m/s)	-2450000	(m/s)	(m/s)
5052.8320	24262.99	46.17	5256.5331	24342.01	35.92
5053.9449	24398.12	26.57	5258.5279	24461.25	33.87
5054.9025	24388.69	26.20	5262.5458	24312.08	39.98
5056.7834	24447.32	31.11	5268.5034	24367.11	33.39
5057.9442	24257.13	20.34	5349.9353	24151.48	35.26
5060.8739	24280.16	21.22	5351.9288	24351.42	26.78
5063.8340	24418.54	41.10	5357.9251	24358.36	50.76
5064.8816	24338.95	28.32	5358.9292	24410.18	36.79
5068.8975	24302.92	34.02	5396.8522	24319.13	45.60
5071.9278	24242.14	22.27	5399.8478	24342.35	40.48
5072.9043	24306.86	24.57	5400.9186	24334.94	34.61
5073.7695	24300.97	24.45	5401.8807	24423.26	29.23
5074.9106	24317.19	28.81	5402.8758	24473.63	38.74
5075.8276	24375.46	30.57	5403.8058	24401.82	37.24
5107.7807	24126.26	44.43	5404.8730	24261.93	41.39
5108.8472	24079.34	39.29	5405.8598	24302.11	35.31
5109.7623	24143.82	30.85	5407.8695	24314.65	34.22
5109.7800	24221.74	27.24	5430.8126	24397.33	32.08
5110.7724	24281.43	29.66	5432.7291	24217.71	40.97
5112.7689	24325.34	28.45	5434.8370	24277.26	30.19
5112.7808	24281.70	29.68	5436.8532	24391.30	29.11
5113.7627	24226.34	32.90	5437.8192	24431.76	34.17
5164.7436	24276.41	29.50	5491.5926	24425.56	46.26
5166.7405	24373.37	34.20	5492.7290	24320.54	42.54
5167.6315	24342.35	32.31	5493.7936	24351.56	32.04
5168.6411	24288.16	21.91	5494.8416	24371.35	37.64
5170.7375	24230.07	34.85	5497.8011	24298.56	30.49
5172.6838	24297.89	41.50	5521.6567	24476.62	22.33
5174.6691	24319.12	26.32	5523.6496	24471.39	25.01
5181.5403	24428.12	32.69	5524.5791	24387.17	17.30
5198.5285	24328.64	35.72	5525.6558	24390.15	17.25
5199.6074	24340.87	28.77	5526.6492	24439.61	15.05
5200.6219	24390.29	30.19	5527.6314	24449.32	25.68
5201.5849	24400.51	21.81	5583.6321	24489.01	14.01
5202.6165	24441.51	25.55	5584.5958	24630.11	21.68
5203.5918	24288.39	30.66	5585.6161	24437.91	36.76
5204.6389	24263.70	31.88	5587.6035	24290.41	50.00
5254.5427	24299.59	41.61	5588.6275	24391.65	66.95
5255.5272	24402.04	40.17			

Larson (1993), where Ca II  $\lambda 8662$  was used to determine the stellar rotation period. Setiawan et al. (2010), for example, used the equivalent width (EW) variations of Ca II  $\lambda 8498$  as a stellar activity indicator to estimate a stellar rotation period that agrees with the bisector analysis.

The EW variation of Ca II  $\lambda 8498$  of HIP 11952 indeed shows a periodic variation with  $P = 1.76$  d with a FAP of few percent. Thus, it is only marginally significant. Following Larson (1993) we then measured the EW variation of Ca II  $\lambda 8662$ . Interestingly, we found a significant periodicity in the EW variation of Ca II  $\lambda 8662$ . The signal corresponds to a peak at a period of  $P = 4.82$  d with FAP =  $8 \times 10^{-3}$ . Fig. 6 shows the EW variation and GLS periodogram of the Ca II  $\lambda 8662$  line. Assuming that this feature is related to the stellar magnetic activity caused by starspots, the period is most-likely linked to the stellar rotation.

### 3.3.3. Photometric data

Photometric V band observations of HIP 11952 are available in the Hipparcos catalogue. Unfortunately, the data set is very sparse, with 72 photometric measurements over a time span

of 893 d. The minimum time-interval between data points is  $\approx 0.014$  d, and the typical photometric errors are  $\approx 0.02$  mag. Due to long-term gaps of several days in the data set, periodicities of a few days cannot be reliably detected. The sampling allows for the detection of very short-term (few hours) as well as long-term (20 d) variations.

We searched for periodicity in the photometric data using a combination of two periodogram analysis techniques: the Scargle periodogram (Scargle 1982) and the CLEAN algorithm (Roberts 1987). The combination of these two techniques provides a reliable period detection as outlined in several rotational period and variability studies (e.g., Rodríguez-Ledesma et al. 2009).

Based on the Scargle periodogram, we detected significant signals at  $P_1 = 0.072$ ,  $P_2 = 0.33$  and at  $P_3 = 2$  d. When the CLEAN algorithm is applied, the 2 d signal is removed and therefore, we concluded that it is probably a false peak or alias due to the clumpy data sampling. Both the 0.072 and 0.33 d periods in the power spectrum remains (Fig. 7), with FAP, based on the Scargle periodogram, of 0.5% and 1%, respectively. All other peaks in Fig. 6 have larger FAPs. We

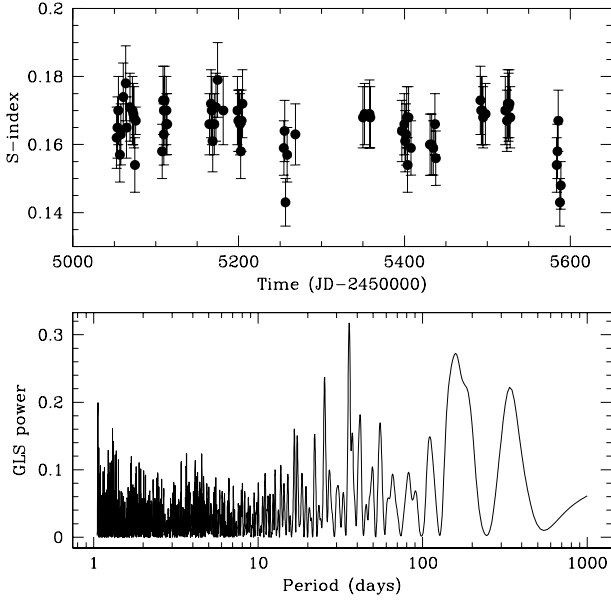


**Fig. 5.** Upper panel: The measurements of Ca II  $\lambda 3934$  S-index. Lower panel: The GLS periodogram of Ca II  $\lambda 3934$  shows a clear peak corresponding to a period of  $P = 36$  d. However, the error bar of the individual measurement is large and the period is close to the observational time window of about 1 month.

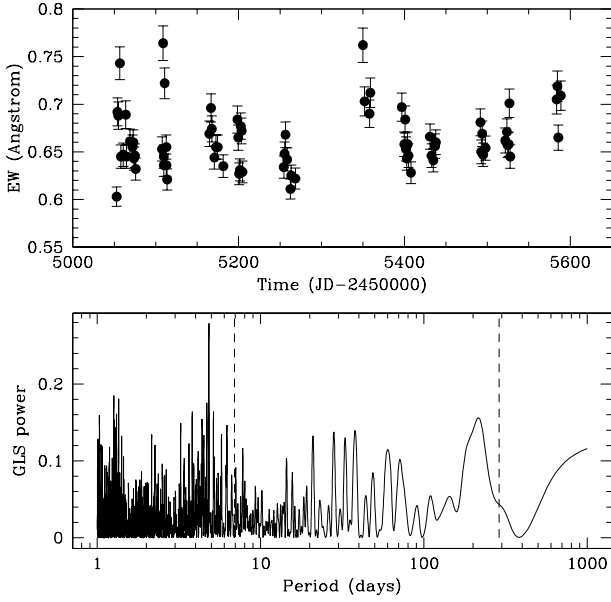
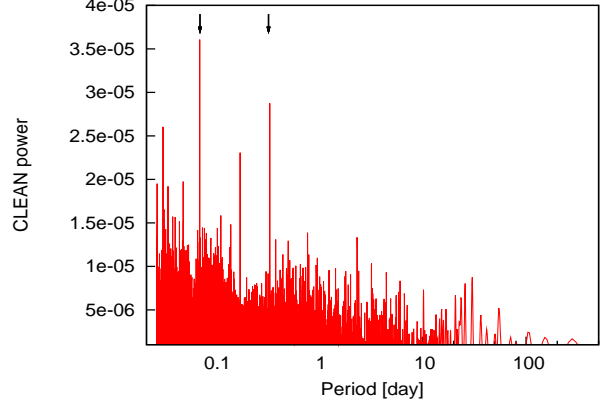


**Fig. 6.** Upper panel: The measurements of Ca II  $\lambda 8662$  EW variation. Lower panel: The GLS periodogram of Ca II  $\lambda 8662$  shows a clear peak corresponding to a period of  $P = 4.82$  d. The dashed line shows the period of the RV variations.

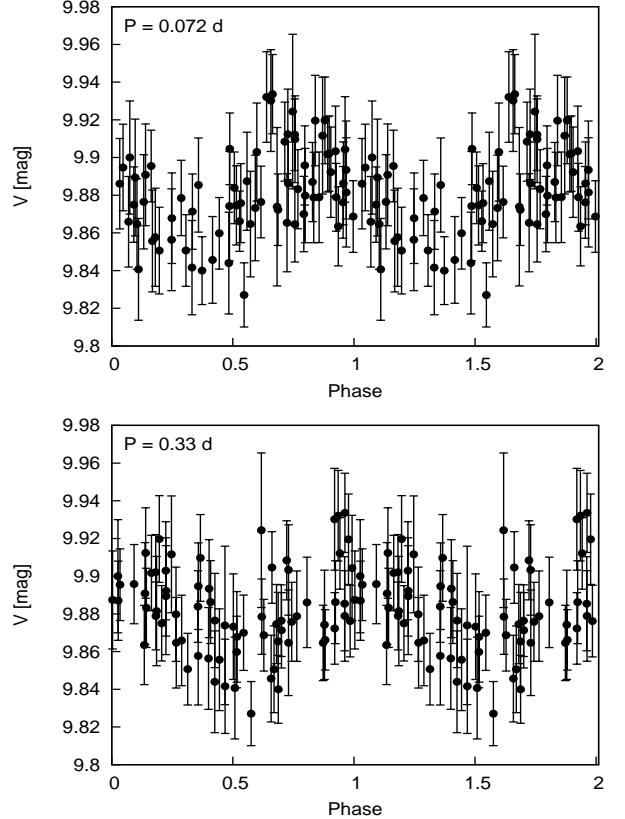
have also computed the statistical F-test and a derived FAP from it (Scholz et al. 2004 and Rodríguez-Ledesma et al. 2009). The  $FAP_{Ftest}$  represents the probability that the period found is caused by variations in the photometric noise, and therefore it is independent of the periodogram analysis. The FAP Ftest derived for the 0.072 and 0.33 d detected peaks are 5 % and 11 %, respectively.

Fig. 8 shows the phase folded light curves with the periods of 0.072 and 0.33 d.

Due to the quality of the data set, however, it is difficult to ensure the significance of these periods. Our analysis suggests some evidence for short-term photometric variations, which might be interpreted as possible pulsation modes in this F-type star.



**Fig. 7.** The photometric observations of HIP 11952 show two peaks at  $P = 0.3$  and  $P = 0.072$  d.



**Fig. 8.** Phase folded light curves from the Hipparcos photometric data.

Based on the analysis of the stellar activity indicators, we assume a stellar rotation period of 4.8 d, as derived from the Ca II

λ8662. Additionally, there might be evidence for stellar pulsations with intra-day periodicities

#### 4. Planetary companion

Since the long-period and short-period RV variations have different characteristics from those of the stellar activity indicators, we concluded that they are most likely caused by the presence of unseen companions.

We computed the orbital solution by using a two-components Keplerian model. In Fig. 9 we show the calculated orbital fit and residual velocities. The orbital parameters are given in Table 3. With a derived primary mass of  $0.83 M_{\odot}$ , we calculated the minimum masses of the companions  $m_2 \sin i = 0.78 M_{\text{Jup}}$  for the inner and  $m_2 \sin i = 2.93 M_{\text{Jup}}$  for the outer companion. The orbital semi-major axes are 0.07 AU and 0.81 AU, respectively. The planetary orbits have moderate eccentricities of 0.35 and 0.27, which seem to be not unusual, based on the statistics of the eccentricity of exoplanets (see e.g., www.exoplanet.eu).

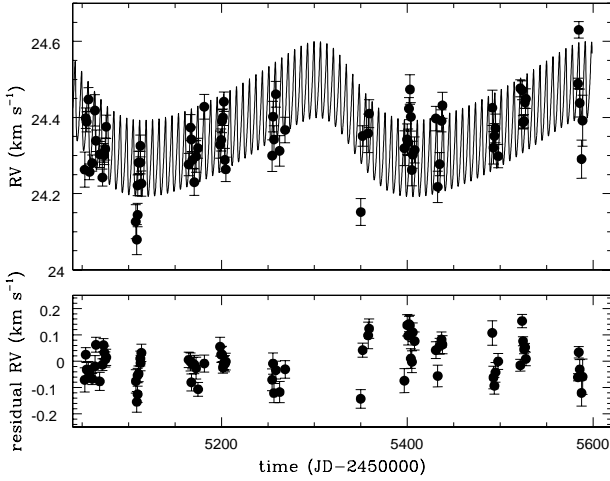


**Fig. 9.** Orbital solution of a two-planets Keplerian fit (upper panel). The orbital parameters are listed in Table.3. The residual velocities are shown in the lower panel.

**Table 3.** Orbital parameters for HIP 11952 b and c

Parameter	Unit	HIP 11952b	HIP 11952c
$P$	d	$290.0 \pm 16.2$	$6.95 \pm 0.01$
$T_0$	JD	$5402.0 \pm 1.3$	$5029.2 \pm 0.04$
	-2450000		
$e$		$0.27 \pm 0.10$	$0.35 \pm 0.24$
$\omega_1$	deg	$59.3 \pm 2.5$	$61.2 \pm 6.6$
$K_1$	$\text{m s}^{-1}$	$105.2 \pm 14.7$	$100.3 \pm 19.4$
$m_2 \sin i$	$M_{\text{Jup}}$	$2.93 \pm 0.42$	$0.78 \pm 0.16$
$a$	AU	$0.81 \pm 0.02$	$0.07 \pm 0.01$
$V_0$	$\text{km s}^{-1}$	$24.365 \pm 0.01$	
$\sigma(O - C)$	$\text{m s}^{-1}$	70.22	
reduced $\chi^2$		1.3	

When calculating the orbital solutions, we obtained a relatively large  $\sigma(O - C)$  value. A possible explanation to this is the

presence of another unseen companion or RV jitter due to the interaction between the two companions. Because of the absence of the emission cores in Ca II H & K, the large  $\sigma(O - C)$  is most likely not due to the intrinsic stellar variability.

We investigated the residual velocities and found a significant signal at  $\sim 40$  days. However, the amplitude of the residual RV variations is in the order of the error bars. Moreover, the window function shows also a peak close to this period. To detect further low-amplitude RV variations, more intensive high-precision RV measurements are needed.

From the knowledge of  $P_{\text{rot}} / \sin i = 15.7$  d (Table 1) and the rotation period  $P = 4.82$  d, we derived an inclination angle of the stellar rotation of  $18^\circ$ . Assuming that the orbital inclination of the companion does not differ much from the stellar rotation inclination angle, we estimated true companion masses of  $2.5$  and  $9.5 M_{\text{Jup}}$ .

#### 5. Discussion

A fundamental parameter of HIP 11952 is the stellar metallicity. The metallicity issue here is particularly interesting, since according to the theory of planet formation via core-accretion processes, planetary companions around such metal poor stars like HIP 11952 are not expected. The majority of the planet host main-sequence stars are metal rich (Fig. 10, upper panel).

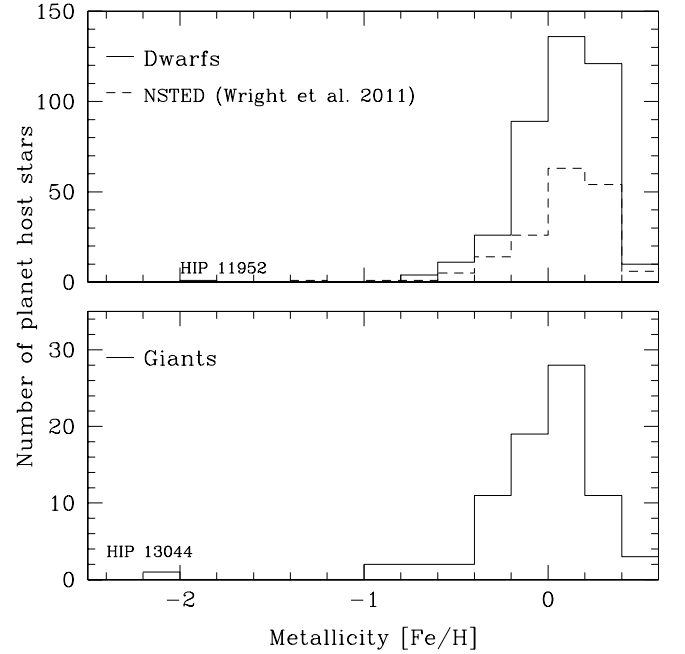


**Fig. 10.** The metallicity distribution of stars hosting planets. Solid lines in the top and bottom panels represent dwarfs and giants, respectively (data from the exoplanet encyclopedia www.exoplanet.eu). Dash lines show data from the exoplanet orbit database (Wright et al. 2011) which does not discriminate between dwarf and giant stars.

For dwarf stars, the metallicity generally reflects the initial metallicity at star formation. Assuming that HIP 11952 is a dwarf or a turn off star, its initial low metallicity makes HIP 11952 unusual among the planetary systems discovered so far (Fig. 10).

The both planetary companions around HIP 11952 belong to only few planets that have been discovered in low metallicity systems ( $[\text{Fe}/\text{H}] < -1.5$ ), comparable to HIP 13044 reported by Setiawan et al. (2010). Note that, so far also only few planets have been detected with host star's metallicities  $-1 < [\text{Fe}/\text{H}] < -0.5$ . This group includes  $\sim 60\%$  main-sequence and  $\sim 40\%$  giants. From the current statistics, about 50% of the giant planet-host stars have sub-solar metallicities.

Whether the metallicity of a giant reflects its initial metallicity is still under debate. The convective envelopes in giant star are much more extended than in main-sequence stars (e.g. Pasquini et al. 2007) and they might alter their surface chemical abundances.

The presence and formation of planets around metal-poor stars, in particular those with metallicities  $[\text{Fe}/\text{H}] < -1.5$  are still poorly understood. According to the core accretion theory (e.g., Safronov 1969; Pollack et al. 1996) high metallicity is required for the formation of planets. Alternatively, planets around metal-poor stars could form by gravitational disk instability processes (e.g., Boss 1998) or other mechanisms (see e.g., Nayakshin 2011). According to Nayakshin (2011) planets around such metal-poor stars have no solid cores and may form as a result of the second collapse (H2 disassociation) of their embryos and radial migrations. Further discoveries of planets around metal-poor stars can provide more constraints on currently different planet formation theories.

The planets around HIP 11952 have orbits with moderate eccentricities. To examine the dynamical stability of the system, numerical simulations are necessary to find stable planetary configurations, see e.g., Barnes & Quinn (2004). Following their calculations, systems with two or more planets in large separated orbits are fully stable. The orbits of HIP 11952 b and c are in a 42:1 ratio and thus far beyond the 10:1 resonance. Therefore, the system HIP 11952 is most likely fully stable.

Finally, HIP 11952 and its planets are among the oldest planetary systems known. HIP 11952 is also older than typical stellar ages in the Galactic thick disk. A possible connection to a metal-poor stellar stream reported by Arifyanto & Fuchs (2006) is an interesting aspect since it suggests that HIP 11952 might actually belong to a part of the thick disk that has been accreted from a disrupted former satellite galaxy, similar to HIP 13044. The age estimation of  $12.8 \pm 2.6$  Gyr given by Feltzing et al. (2001) is 1 Gyr older than that of HD 114752 which has an estimated age of  $11.8 \pm 3.9$  Gyr. HIP 11952's age is close to the one of HE 1523-0901, which is the oldest star ( $13.2 \pm 2.7$  Gyr) known so far (Frebel et al. 2007). The old stellar age is supported by the very low metallicity of HIP 11952 which is typical of Population II stars.

## 6. Conclusions

We observed RV variations of HIP 11952. The spectroscopic and photometric analysis of the star show that the periodic RV variations are not caused by the intrinsic stellar variability. Based on our analysis, we detected two planetary companions around the metal poor star HIP 11952 with orbital periods of 6.95 d and 290 d. We found evidence for intra-day stellar pulsations and observed a stellar rotation of 4.82 d. We computed the companion's minimum mass of  $m_2 \sin i = 0.78 M_{\text{Jup}}$  for the inner planet and  $m_2 \sin i = 2.93 M_{\text{Jup}}$  for the outer one. Additional high-precision RV measurements are necessary to improve the orbital solution and put more constraints on the eccentricities. Further RV observations might also reveal the presence of other low-mass companions in the system. From the metal abundance analysis that

we carried out, we obtained an average  $[\text{Fe}/\text{H}] = -1.90 \pm 0.06$  from Fe I and Fe II, respectively, which makes HIP 11952 b and c the first planets discovered around a dwarf or subgiant star with  $[\text{Fe}/\text{H}] < -1.5$ . This discovery is also remarkable since the planetary system most likely belong to the first generation of planetary systems in the Milky Way.

*Acknowledgements.* We thank N. Christlieb for the support and useful discussions. We also thank A. Mueller, M. Zechmeister, J. Carson, W. Wang, C. Ruhlmann, T. S. Hartung, S. Albrecht, R. Lachaume and T. Anguita for observing HIP 11952 with FEROS.

## References

- Arifyanto, M. I., & Fuchs, B., 2006, *A&A*, 449, 533  
 Barnes, R. & Quinn, Th., 2004, *ApJ*, 611, 494  
 Bessell, M. S., 2000, *PASP*, 112, 961  
 Bouchy, F., et al. 2010, *A&A*, 519, A98  
 Boss, A. P., 1998, *ApJ*, 503, 923  
 Caffau, E., Ludwig, H.-G., Steffen, M., Freytag, B., & Bonifacio, P., 2011, *Sol. Phys.*, 268, 255  
 Caffau, E., Ludwig, H.-G., Steffen, M., Freytag, B., & Bonifacio, P., 2010, *Sol. Phys.*, 66  
 Casagrande, L., Ramírez, I., Meléndez, J., Bessell, M., & Asplund, M., 2010, *A&A*, 512, A54  
 Cayrel de Strobel, G., Soubiran, C., Friel, E. D., et al. 1997, *A&A*, 124, 299  
 Cayrel de Strobel, G., Soubiran, C., Ralite, N., 2001, *A&A*, 373, 159  
 Carney, B. & Latham, D., 1987, *AJ*, 93, 116  
 Cenarro, A. J., et al. 2007, *MNRAS*, 374, 664  
 Charbonnel, C. & Primas, F., 2005, *A&A*, 442, 961  
 de Medeiros, J. R., & Mayor, M., 1999, *A&AS*, 139, 433  
 Eggen, O. J. & Sandage, A. R., 1959, *MNRAS*, 119, 225  
 Edvardsson, B., Andersen, J., Gustafsson, B., Lambert, D. L., Nissen, P. E., & Tomkin, J., 1993, *A&A*, 275, 101  
 Feltzing, S., Holmberg, J., & Hurley, J. R., 2001, *A&A*, 377, 911  
 Fischer, D. A., & Valenti, J., 2005, *ApJ*, 622, 1102  
 Fouts, G., 1987, *PASP*, 99, 986  
 Frebel, A., Christlieb, N., Norris, J. E., et al. 2007, *ApJ*, 660, L117  
 Fulbright, J. P., 2002, *AJ*, 123, 404  
 Girardi, L., et al. 2010, *ApJ*, 724, 1030  
 Gratton, R. G., Carretta, E., & Castelli, F. 1996, *A&A*, 314, 191  
 Gray, R. O., & Corbally, C. J., 2009, *Stellar Spectral Classification by Richard O. Gray and Christopher J. Corbally*. Princeton University Press, 2009,  
 Hatzes, A. P., 1996, *PASP*, 108, 839  
 Johnson, J. A., Aller, K. M., Howard, A. W. & Crepp, J. R., 2010, *PASP*, 122, 905  
 Kaufer, A., & Pasquini, L., 1998, *Proc. SPIE*, 3355, 844  
 Kharchenko, N. V., & Roeser, S., 2009, *VizieR Online Data Catalog*, 1280, 0  
 Klement, R. J., 2010, *A&A Rev.*, 18, 567  
 Kurucz, R., 1993, *ATLAS9 Stellar Atmosphere Programs and 2 km/s grid*. Kurucz CD-ROM No. 13. Cambridge, Mass.: Smithsonian Astrophysical Observatory, 1993, 13  
 Kurucz, R. L. 2005, *Memorie della Societa Astronomica Italiana Supplementi*, 8, 14  
 Larson, A. M., Irwin, A. W., Yang, S. L. S., et al. 1993, *PASP*, 105, 332  
 Marigo, P., Girardi, L., Bressan, A., Groenewegen, M. A. T., Silva, L., & Granato, G. L., 2008, *A&A*, 482, 883  
 Masana, E., Jordi, C. & Ribas, I., 2006, *A&A*, 450, 735  
 Minchev, I., Quillen, A. C., Williams, M., Freeman, K. C., Nordhaus, J., Siebert, A., & Bienaymé, O., 2009, *MNRAS*, 396, L56  
 Nayakshin, S., 2011, arXiv 1102.4297  
 Pasquini, L., Döllinger, M. P., Weiss, A., Girardi, L., Chavero, C., Hatzes, A. P., da Silva, L., & Setiawan, J., 2007, *A&A*, 473, 979  
 Perryman, M. A. C., & ESA, 1997, *ESA Special Publication*, 1200,  
 Pollack, J. B., Hubickyj, O., Bodenheimer, P., et al., 1996, *Icarus*, 124, 62  
 Roberts, D. H., & Dreher, J. W., 1987, *AJ*, 93, 968  
 Rodríguez-Ledesma, M. V., Mundt, R., & Eisloffel, J., 2009, *A&A*, 502, 883  
 Sánchez-Blázquez, P., Peletier, R. F., Jiménez-Vicente, J., 2006, *MNRAS*, 371, 703  
 Safronov, V. S., 1969, *Evolutsiia do planetnogo oblaka*  
 Santos, N. C., Mayor, M., Naef, D., et al. 2000, *A&A*, 361, 265  
 Santos, N. C., et al. 2010, *A&A*, 512, A47  
 Santos, N. C., et al. 2011, *A&A*, 526, A112  
 Sbordone, L., 2005, *Memorie della Societa Astronomica Italiana Supplementi*, 8, 61



- Sbordone, L., Bonifacio, P., Castelli, F., & Kurucz, R. L., 2004, *Memorie della Societa Astronomica Italiana Supplementi*, 5, 93
- Scargle, J. D., 1982, *ApJ*, 263, 835
- Scholz, A. & Eislöffel, J., 2004, *A&A*, 421, 259
- Setiawan, J., Pasquini, L., da Silva, L., von der Lühe, O., & Hatzes, A., 2003, *A&A*, 397, 1151
- Setiawan, J., Klement, R. J., Henning, T., Rix, H.-W., Rochau, B., Rodmann, J., & Schulze-Hartung, T., 2010, *Science*, 330, 1642
- Simpson, E. K., Barros, S. C. C., Brown, D. J. A. et al. 2011, *AJ*, 141, 8
- Sivarani, T., et al. 2004, *A&A*, 413, 1073
- Sozzetti, A., Torres, G., Latham, D. W., Stefanik, R. P., Korzennik, S. G., Boss, A. P., Carney, B. W., & Laird, J. B., 2009, *ApJ*, 697, 544
- Valdes, F., Gupta, R., Rose, J. A., Singh, H. P., & Bell, D. J., 2004, *ApJS*, 152, 251
- Valenti, J. A. & Fischer, D. A., 2005, *ApJS*, 159, 141
- Vaughan, A. H., Preston, G., W. & Wilson, O. C., 1978 *PASP*, 90, 267
- Wright, C. O., Egan, M. P., Kraemer, K. E., & Price, S. D., 2003, *AJ*, 125, 359
- Wright, J. T., Fakhouri, O., Marcy, G. W. et al., 2011, *PASP*, 123, 412
- Zechmeister, M., Kürster, M., 2009, *A&A*, 496, 577
- Zerbi, F. M., 2000, *Delta Scuti and Related Stars ASP Conference Series*, 210, 332